Geol. Bull. Univ. Peshawar, Vol. 38, pp. 65-79, 2005

Kinematics of tectonic fracture development during regional folding in sandstones of the Kamlial Formation, Khushalgarh, northern Pakistan

MOHAMMAD SAYAB[1] & QUAID K. JADOON[2]
[1]National Centre of Excellence in Geology, University of Peshawar.
[2]LMK Resources, ETC building, Sir Agha Khan Road, F-5/1, Islamabad.

ABSTRACT: *Systematic relationships between the fracture orientation and fold geometry in sedimentary rocks have been used to explain the development of synfolding fractures. Based on field observations at the Khushalgarh syncline, located east of the Kohat plateau, we proposed that the orientation of fractures was influenced dominantly by two tectonic fracture sets, that is, the NE-SW and NW-SE. The NE-SW fracture set dominantly formed as mode I (tensile), where as, the NW-SE fracture set developed as mode II (shear) conjugate fractures. The NE-SW trending fractures follow the axis of the syncline, whereas, the NW-SE fracture set crosscuts the fold axis. Most of the NE-SW fractures abut against the NW-SE fracture set. Based on the orientation and crosscutting relationships, their modes in response to stress, we conclude that the NE-SW trending fractures formed early than those of NW-SE fracture set. Though, both the fracture sets are formed during the folding, we suggest that they were not formed at the same time. Their crosscutting relationship suggests that they developed sequentially rather than synchronously. Our interpretations support the laboratory-based models where only one fracture orientation (or set of fractures with one orientation) form in response to single stress. However, as the stress distribution in folded strata changes over time, new fractures of distinct orientations can form during or late in the folding history. We conclude that the sandstone units underwent bedding-parallel extension during folding, where bedding is stretched to accommodate extension, parallel to the fold axis orientation. Bending of the limbs is a likely mechanism for the development of observed NE-SW trending fractures during folding, whereas the NW-SE fractures developed late in the folded history.*

INTRODUCTION

Foreland fractured sedimentary rocks are known to carry important aquifers and hydrocarbon reservoirs (e.g., Dholakia et al., 1998). Despite a vast literature on rock fractures, their geometrical characteristics in folded sedimentary rocks are still poorly known (e.g., Billi & Salvini, 2003). Yet, understanding of fractures in relation to folded stress regime can provide pathways to facilitate hydrocarbon exploration. In recent years, tectonic fractures in sedimentary rocks have received much attention because they often preserved pre-, syn- or post-tectonic histories of foreland terranes (e.g., Billi, in press). Classic fold-fracture model proposed by Stearns (1968) assumes that three possible fracture orientations of five different sets can form systematically with respect to the fold axis and bedding. However, this assumption conflicts experimental work, which suggests

that usually only one fracture orientation form in a rock in response to stress (Griggs & Handin, 1960). Price and Cosgrove (1990) and Twiss and Moores (1992) argued that for any fold-fracture model, a systematic relationship is needed between fracture orientation and fold geometry. These authors envisaged that following criteria should be used to explain the fold-fracture relationship:

1. the spatial distribution of fractures,
2. evidence for tensile and shear displacement across fractures, and
3. the sequence of fracture formation

We have adopted this approach here in this paper. Attributes of fractures and fracture network from the Khushalgarh syncline of the eastern Kohat plateau (Fig. 1a) are qualitatively and quantitatively presented. The area forms a part of the Himalayan foreland fold and thrust belt of northern Pakistan. Fracture patterns across the Khushalgarh syncline show remarkable trends and this data, in relation to the folding, is described below.

LITHOLOGICAL DESCRIPTION

The Miocene Kamlial Formation in the Kushalgarh area consists of fluvial sandstone of the Siwalik Group. Sandstone bodies are grey color, medium to coarse-grained, interbedded with brick-red shale and intra- and extra-formational conglomerates. The sandstone is cross-bedded to massive and moderately to poorly-sorted. Degree of cementation varies from poorly to moderately cemented sandstone. However, highly cemented hard sandstone bands of varying thickness (ranges between ca. 0.1 to 1 m) are frequent within the sandstone.

METHODOLOGY

Fracture data were collected directly from outcrops using conventional structural techniques, that is, inventory circle, scanline and rectangle methods. For simplicity, we have adopted the fracture descriptions proposed by Berg and Skar (in press) as planar to semi-planar discontinuities in a rock mass caused by stress. The data recorded from each station include fracture type and mode, orientation, frequency, geometry and termination (e.g., Berg & Skar, in press). Fracture mode comprises mode I and mode II fractures. In mode I fracturing, fractures are in tensile or opening mode, whereas mode II fracturing are in shear mode. Data have analyzed from one rectangle, one scanline and four inventory circle stations (Fig. 1b).

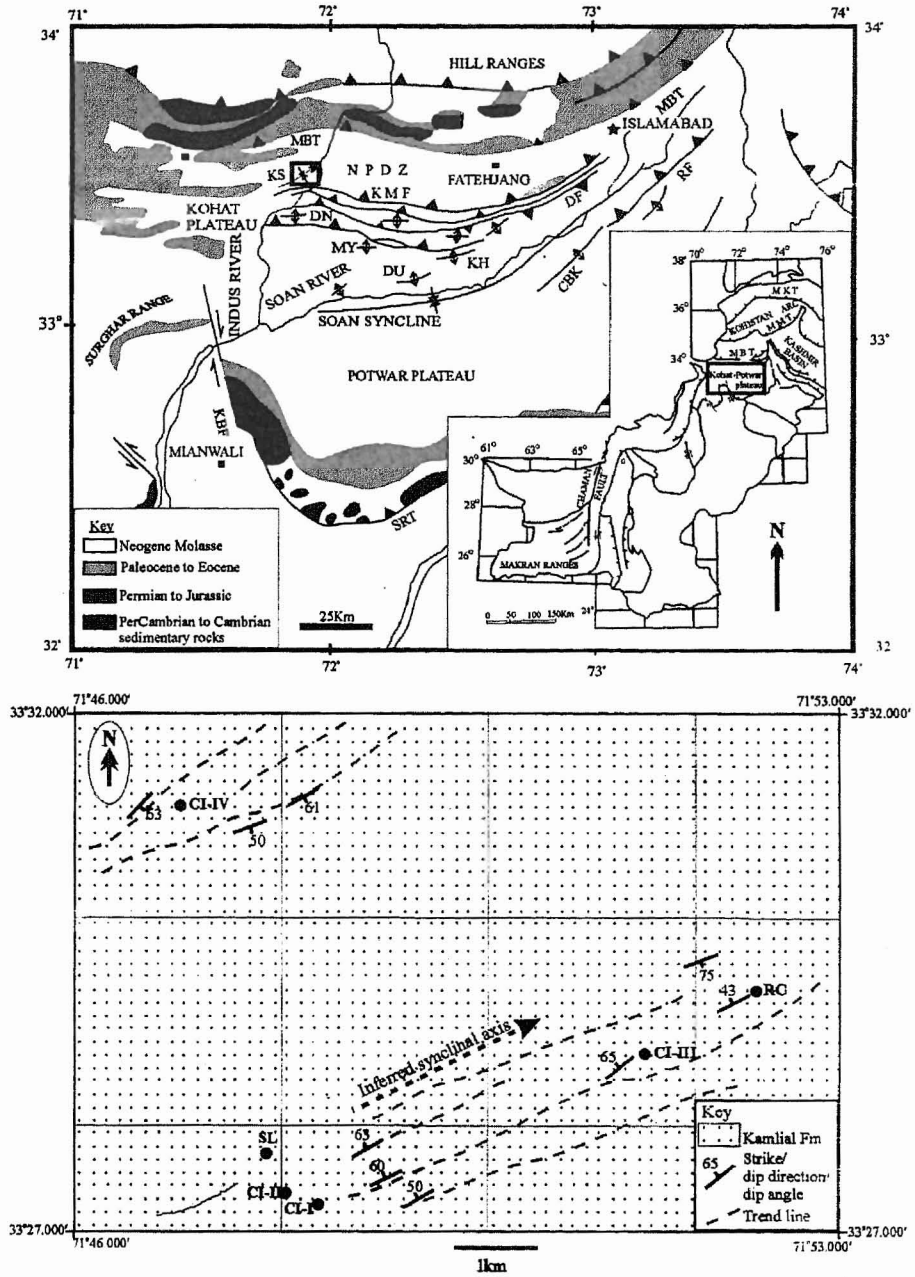

Fig. 1. (a) Generalized map of the Kohat, Potwar and Salt Range showing prominent tectonic features (after Jaswal et al., 1997). KS (Khushalgarh syncline (after Searle and Khan, not dated).

CBK=Chak Beli Khan anticline, DF=Dhurnal Fault, DJ=Dil Jabba Fault, DN=Dakhni anticline, DU=Dhulian anticline, KBF=Kalabagh Fault, KH=Khaur anticline, KMF=Kheri Murat Fault, MBT=Main Boundary Thrust, MY=Meyal anticline, RF=Riwat Fault, SRT=Salt Range Thrust.

(b) Simplified geological map of the study area showing locations where fracture data was collected. CI: circle inventory, SL: scanline, RC: rectangle.

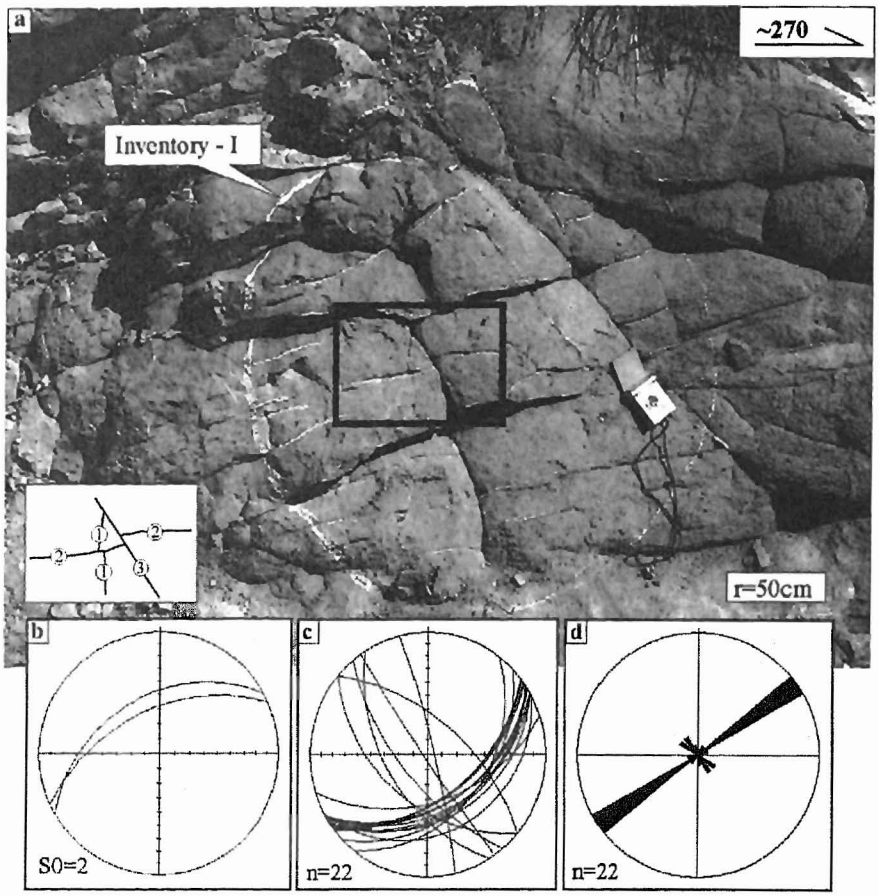

Fig. 2. (a) Photograph of fractures and inventory station 1. (b) Lower hemisphere equal-area stereo plot of bedding (S0) and (c) fractures. (d) Rose diagram showing trends of the fractures.

INVENTORY CIRCLE METHOD

Inventory circle I

At inventory station I (33° 27.233 N; 71° 48.366 E) the strike of the bedding (S0) is ENE-WSW, moderately dipping towards NNW (Fig. 2). The inventory circle contains two sets. The dominant set 2, strike NE-SW and moderately dipping towards SE. This set crosscuts the bedding and strikes parallel to the bedding and this relationship is shown in figures 2b and 2c. As the displacement is normal to the discontinuity walls, therefore, they are tensile or extensional fractures. However, shear component along these fractures have locally been observed. The frequency of fracture set 2 (0.16 *f*/meter) is high with respect to the set 1 fractures observed within the inventory circle. Most of the fractures of set 2 are planar or slightly undulating (terminology after Peacock et al., 2000). In terms of fracture connectedness, their ends are free or some show one end connected with set 1. The least dominant set (1) is characterized by steeply dipping fractures striking NW-SE (Fig. 2d). They

cross cut the bedding. The frequency of these fractures is low (0.04 *f*/m) as compared to the set 2. They are slightly undulating and connected with set 2 fractures, therefore, their ends are not free in terms of fracture connectedness. Set 1 appears to be the youngest fracture in the inventory circle as it crosscuts set 2. Calculated fracture density (cumulative length/area) within the inventory circle is 0.10 cm^{-1} (Table 1).

TABLE 1. FRACTURE DENSITY CALCULATIONS

	Inv-I	Inv-II	Inv-III	Inv-IV	Rectangle
F No.	L (cm)	L (cm)	L (cm)	L (cm)	L (cm)
1	99	37	33	83	54
2	96	28	35	48	21
3	38	100	87	13	23
4	81	89	95	64	140
5	67	95	21	10	53
6	36	80	87	52	123
7	37	56	65	30	31
8	13	95	30	37	82
9	28	22	100	87	40
10	42	30	21	87	90
11	76	27	20	42	52
12	15	85	97		22
13	16	56	16		54
14	10	58			21
15	7	38			110
16	10	22			66
17	48	22			50
18	35				40
19	48				90
20	14				19
21	19				45
22					111
23					63
24					142
25					79
26					86
27					63
28					57
Total length	835	940	707	553	1827
Density	0.10cm^{-1}	0.11cm^{-1}	0.09cm^{-1}	0.07cm^{-1}	0.03cm^{-1}

Rectangle area 140 x 390cm=54600cm^2
Radius of circle = 50cm; Area = 7850cm^2

Inventory circle II

At inventory station II (33° 27.242 N; 71° 48.038 E) the strike of the bedding (S0) is ENE-WSW, moderately dipping towards NNW (Figs. 3a & b). The inventory circle contains two dominant sets. Set 1 is bedding parallel and striking NE-SW, moderately dipping towards NW (Fig. 3c). The frequency of fracture set 1 is high (0.11 *f*/m) as compared to set 2. These fractures are mostly planar, mode I, and are connected with set 2 fractures. The set 2 fractures crosscut the bedding and are generally planar and through- going and correspond to mode II fractures. Though, accommodate minor amount of shear displacement, have reverse shear sense. The spacing between the fractures is regular. Fracture density is estimated around 0.11 cm^{-1}.

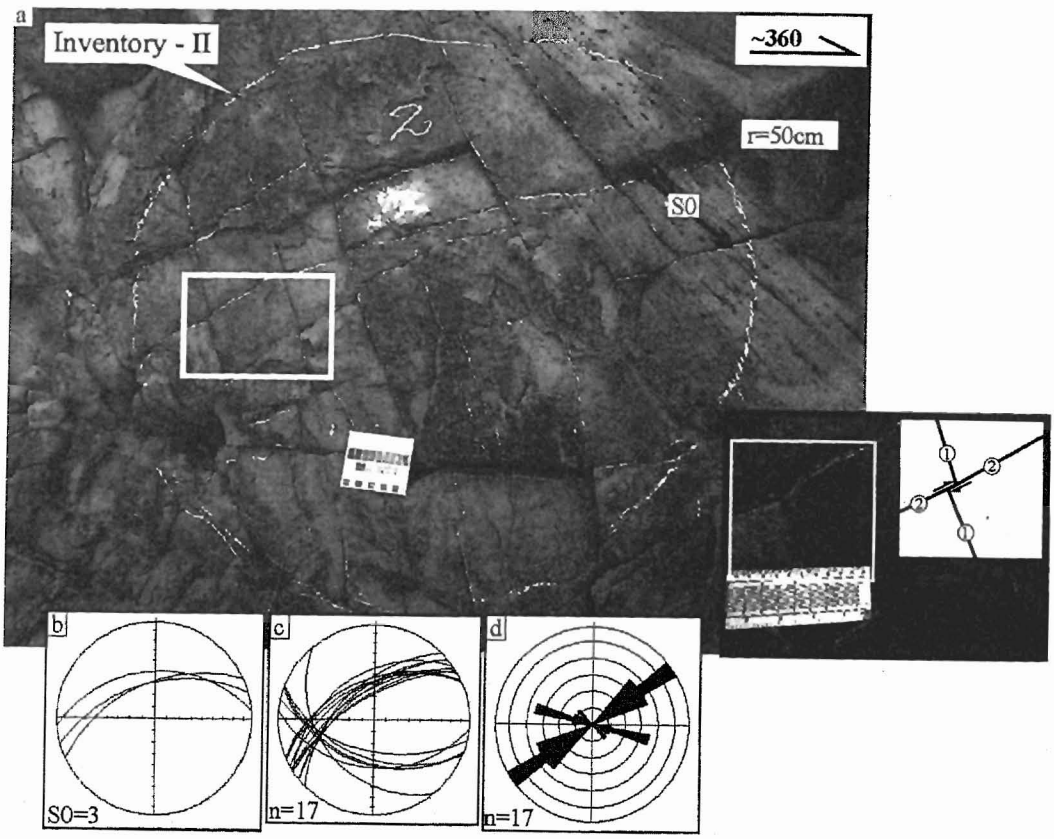

Fig. 3. (a) Photograph of fractures and inventory station II. (b) Lower hemisphere equal-area stereo plot of bedding (S0) and (c) fractures. (d) Rose diagram showing trend of the fracture sets.

Inventory circle III

At inventory station III (33° 28.691 N; 71° 51.534 E), the strike of the bedding (S0) is NE-SW, steeply dipping towards NW (Figs. 4a,b & c). Two fracture sets are recognized. Set 1, dominates in the inventory circle, strikes parallel to the bedding and dipping in the opposite direction with respect to the bedding (cf. Figs. 4c & d). The fractures in this set are evenly spaced and sub-parallel. The frequency of the fractures is 0.07 *f*/m. They are planner to slightly undulating, dominantly mode I, and their ends are connected with set 2 fractures. Set 2 fractures belong to mode II and form a prominent X-type geometry within the inventory circle (Fig. 4a). The frequency of set 2 is low as compared to set 1 and appears to be latest as they displaced set 1 fractures. The shear displacement is minor (<3cm). Calculated fracture density within the inventory circle III is 0.09 cm^{-1}.

Inventory circle IV

At inventory station IV (33° 31.034 N; 71° 47.022 E), the strike of the bedding (S0) is NE-SW, steeply dipping towards SE (Fig. 5c). The inventory contains shallow NW dipping and NE-SW striking set 1 fractures, which are evenly spaced, planar to slightly undulating, subparallel and belong to mode I. The frequency of the set 1 fractures is relatively high (0.08 *f*/m). Set 1 appears to be older as minor (≤2 cm) amounts of slip observed at the intersection of set 1 and fracture labeled 7 in figure 5a. Fracture 7 and 8 form X-type geometrical relationship with infinitesimal displacement. Both fractures are planar and connected with set 1. Density of all the fractures is around 0.07 cm^{-1}

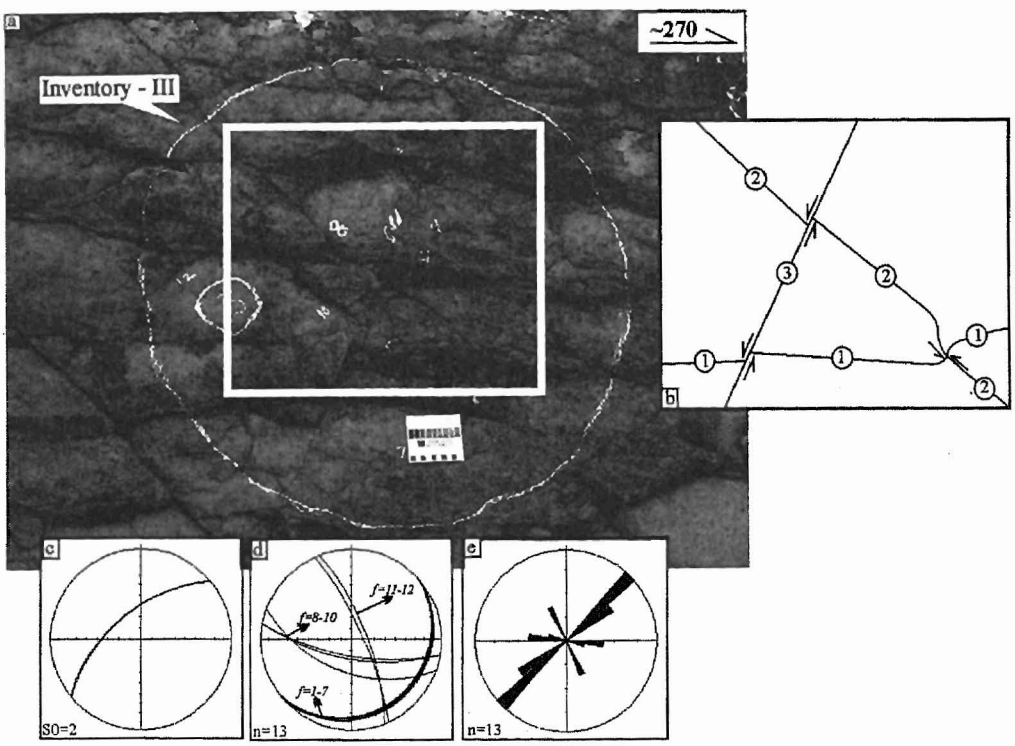

Fig. 4. (a) Photograph of fractures and inventory station III. (b) Cross cutting relationship of fractures and their relative timing. (c) Lower hemisphere equal-area stereo plot of bedding (S0) and (d) fractures. (E) Rose diagram showing trends of the fractures.

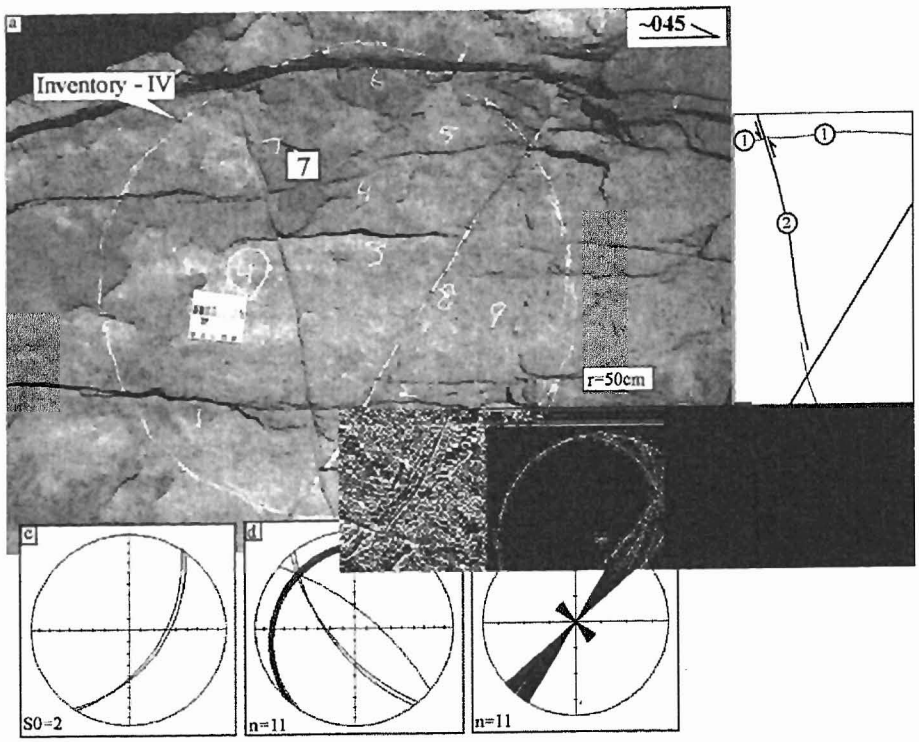

Fig. 5. (a) Photograph of fractures and inventory station IV. (b) Cross cutting relationship of fractures and their relative timing. (c) Lower hemisphere equal-area stereo plot of bedding (S0) and (d) fractures. (e) Rose diagram showing trends of the fractures.

RECTANGLE METHOD

Tectonic fractures were mapped and measured at a rectangle shape outcrop face 33° 29.296 N; 71° 52.574 E) (Fig. 6a). The rectangle was ca. 390 cm long and 140 cm wide. Strike of the bedding (S0), which contains fractures, is NE-SW, moderately dipping towards NW (Fig. 6a). Altogether, 21 fractures were measured of different orientations and lengths. Trends of the fractures were plotted on Rose diagrams (Fig. 6a). The dominant set is NW-SE followed by NE-SW, NS and W-E. The NW-SE trending fractures moderately to steeply dipping either towards NE or SW, whereas NE-SW fractures moderately to shallowly dipping towards SE (Fig. 6b). N-S and E-W trending fractures moderately dipping towards the east and south, respectively (Fig. 6b). The fractures are slightly undulating and their ends are either connected or abut against the younger fractures. It is apparent from the outcrop observations that most of NE-SW fractures are mode I and older than NW-SE fractures, whereas NW-SE fractures correspond to shear or mode II fractures. The NW-SE set fractures are calcite filled with few preserved slip striations. Fracture density within the rectangle is 0.03 cm^{-1}

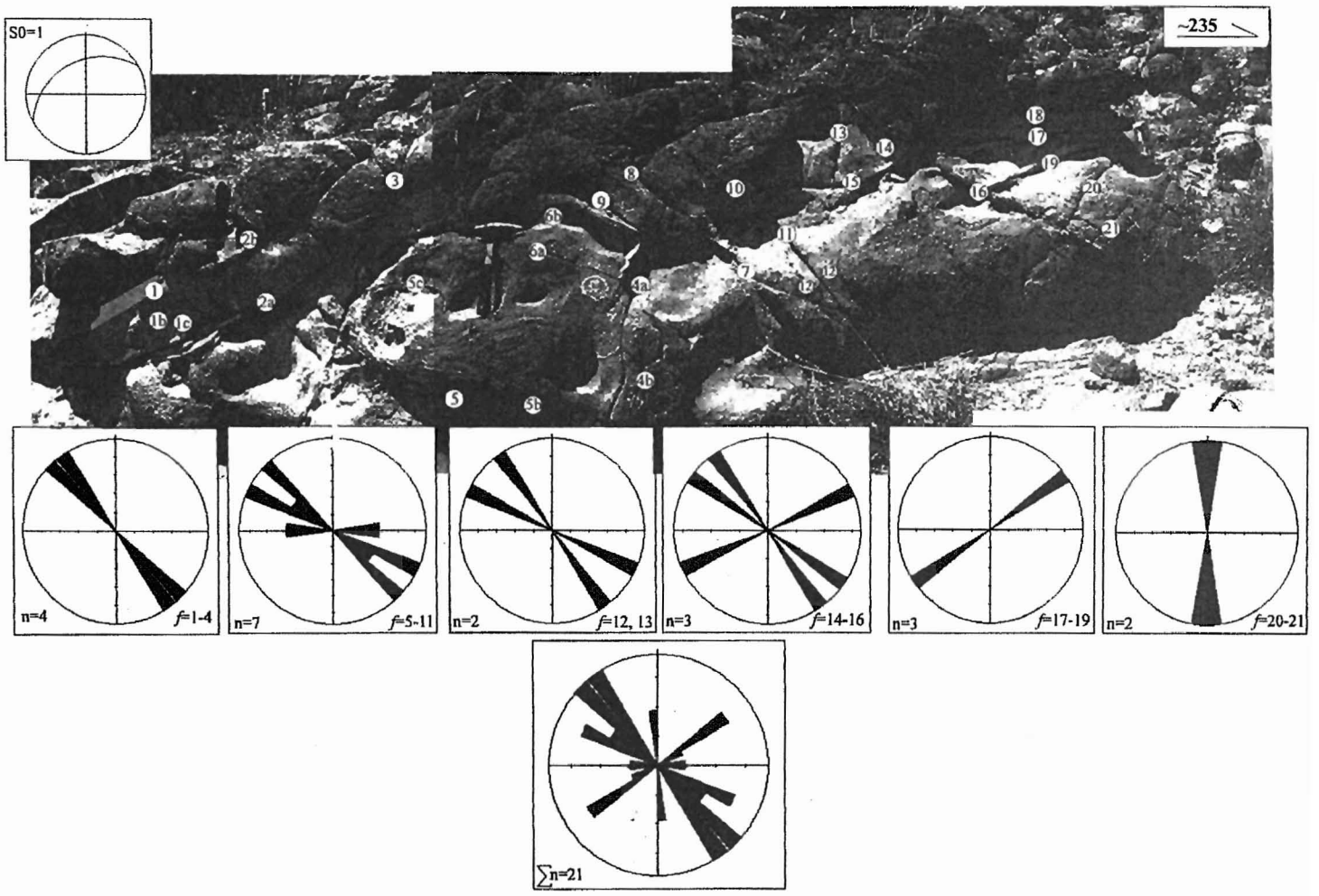

Fig. 6a. Fracture distribution within the rectangle. Rose plots showing the trends of the fractures (see text for description).

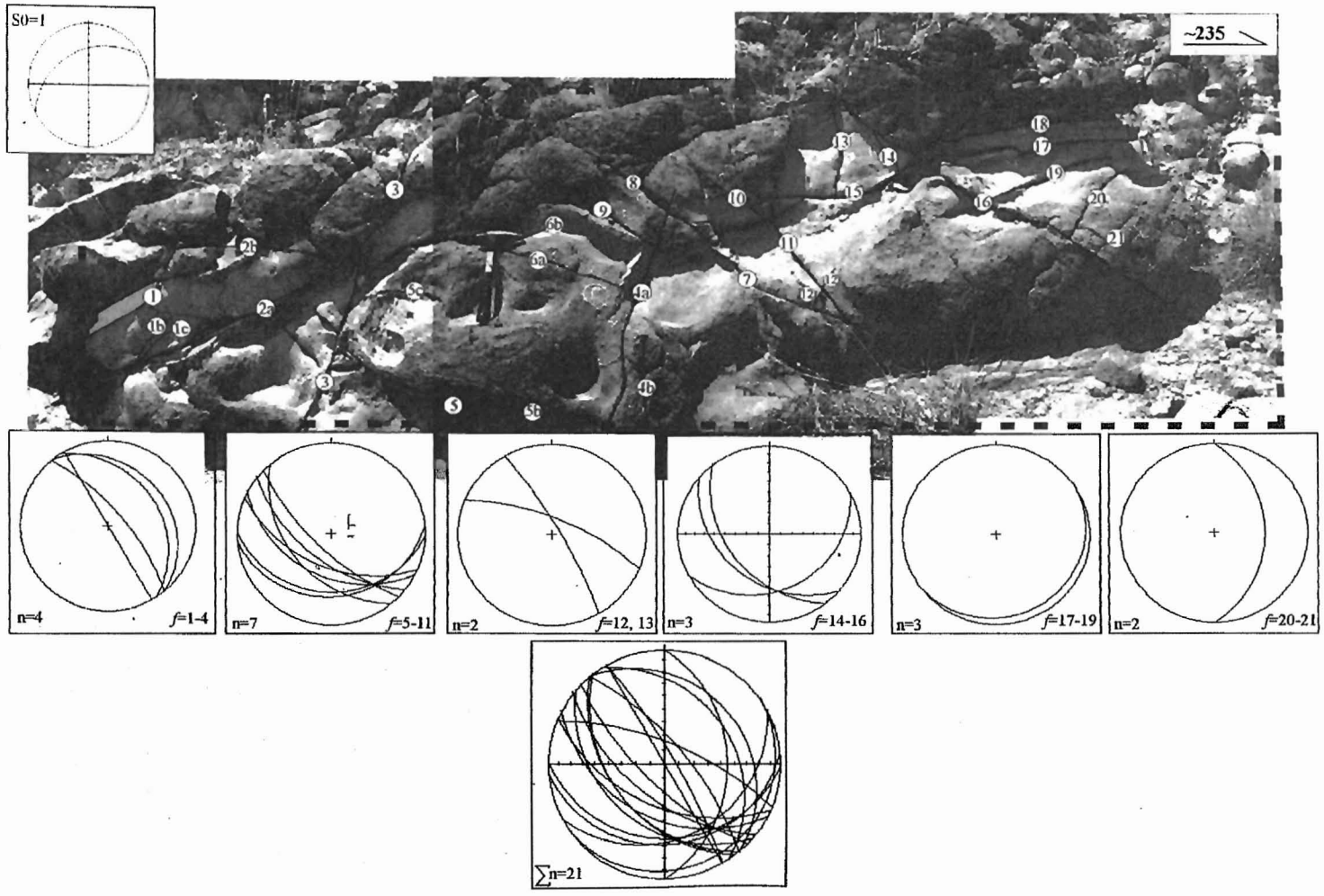

Fig. 6b. Lower hemisphere equal- area stereo plots of fracture distribution within the rectangle (dash box).

SCANLINE METHOD

At location (33° 27.725 N; 71° 47.875 E), dominant N-S striking and steeply dipping fractures were observed (Fig. 7a,c & d). Scanline method was used to collect fracture data (Fig. 7a). A graduated tape was stretched across the outcrop face and setup at near-right angles to the fracture set. The scanline was 260cm (Fig. 7a). The bedding (S0) strikes NE-SW, steeply dipping towards NW (Fig. 7b). 8 major and 2 minor fractures intersect the scanline, and their measurements and fracture properties were recorded. The frequency of the fractures along the scanline is 0.03 *f*/m. Major fractures are near-parallel, through-going and planar. Spacing of the fractures is evenly distributed.

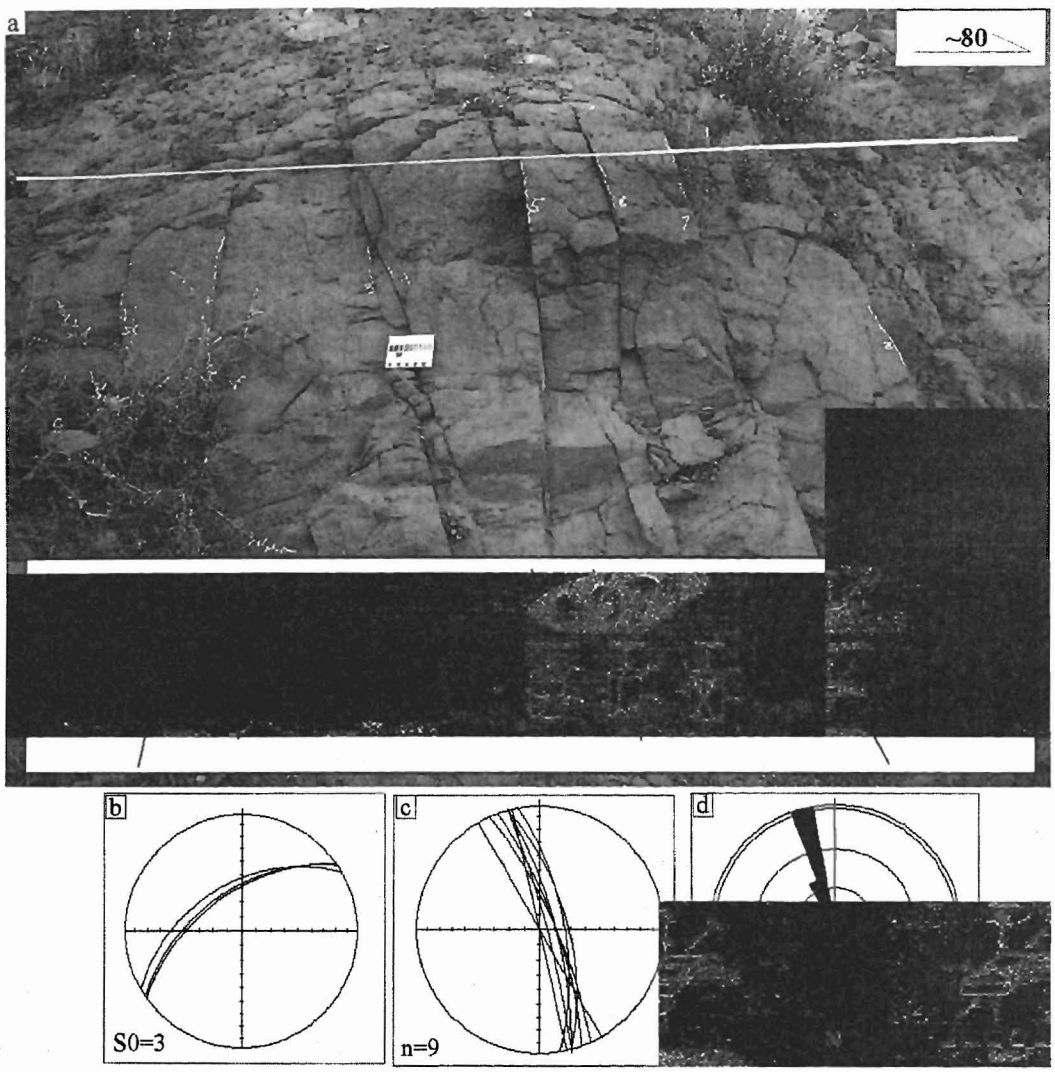

Fig. 7. (a) Photograph showing scanline method for measuring fractures. (b) Lower hemisphere equal-area stereo plot of bedding (S0) and (c) fractures. (d) Rose diagram showing trends of the fractures.

FOLD-FRACTURE RELATIONSHIP: KINEMATIC MODELS

A variety of methods exist in the literature to interpret the geometry of fractures in folded strata (e.g., Stearns, 1968; Price & Cosgrove, 1990). Stearns (1968) suggested that there are five fracture sets that form systematically with respect to the fold axis and bedding and are comprised of two conjugate shear orientations and one extension orientation (Fig. 8a,b). Fracture set 1, resulting from a greatest compressive stress parallel to the dip direction of bedding, includes two orientations with dominantly strike-slip and one extension fracture orientation (Fig. 8a). For fracture set 2, the least compressive stress is parallel to the dip direction. Stearns suggested that the principal stresses and strains are known to exchange orientations across the neutral surfaces subject to pure bending. Because fracture sets are specifically related to bending, their attitudes may change spatially, for example at the nose of a plunging anticline (Fig. 8b). Fracture set 3 is comprised of two orientations of shear fractures, which accommodate normal offset, and one orientation of extension fractures. Set 4 includes two orientations of reverse faults. Stearns suggests that set 1 forms early during folding, set 2 forms when extension normal to the fold becomes "large", and sets 3 and 4 "reflect locally developed bending or buckling". The fifth fracture set is interpreted to be shear fractures that form as a result of bedding plane slip during folding. Thus, in Stearns (1968) fold-fracture model, all four sets are related to the folding of beds. From the concepts developed in figure 8a, Stearns proposed the conceptual model of figure 8b, which illustrates the spatial relationships of fractures on folds. 11 different fracture orientations form within the same folded bed. This conceptual model assumes that all three possible fracture orientations of each set can form. This assumption, however, contradicts laboratory observations suggesting that usually only one fracture orientation form in a sample (e.g., Twiss & Moores, 1992). Griggs and Handin (1960), based on the rock mechanic testing, conclude that extension fractures form perpendicular to the least compressive stress (σ_3). Shear fractures form parallel to the intermediate principal stress (σ_2) and oblique to the greatest compressive stress (Fig. 8c).

Some researches have doubted the applicability of symmetric relationship between fold geometry and the development of fractures. Price and Casgrove (1990) reasoned that if a symmetric relationship cannot be established between fold geometry and fracture orientation, the observed factures did not form during folding. They proposed that fracture-fold relationship assume that the rock was unfractured prior to folding or that fractures formed early during folding. Twiss and Moores (1992) pointed out that fractures on folds can either be pre- syn- or post-date folding. To establish this relationship one should formulate the interpretations of their development based on the evidence for displacement across fractures, the spatial distributions of fractures and the timing or sequence of fracture formation.

FRACTURE DEVELOPMENT IN THE KHUSHALGARH SYNCLINE

Based on the field observations from the Khushalgarh syncline, we interpret fractures of the NE-SW set dominantly formed as mode I fractures (tensile), whereas, fractures of the NW-SE set developed as mode II conjugate fractures (shear). From the field evidences, the sequence of fracture development is straightforward. The NE-SW trending fractures follow the axis of the syncline and abut the NE-SW set (Fig. 9).


2
3
5
4
1

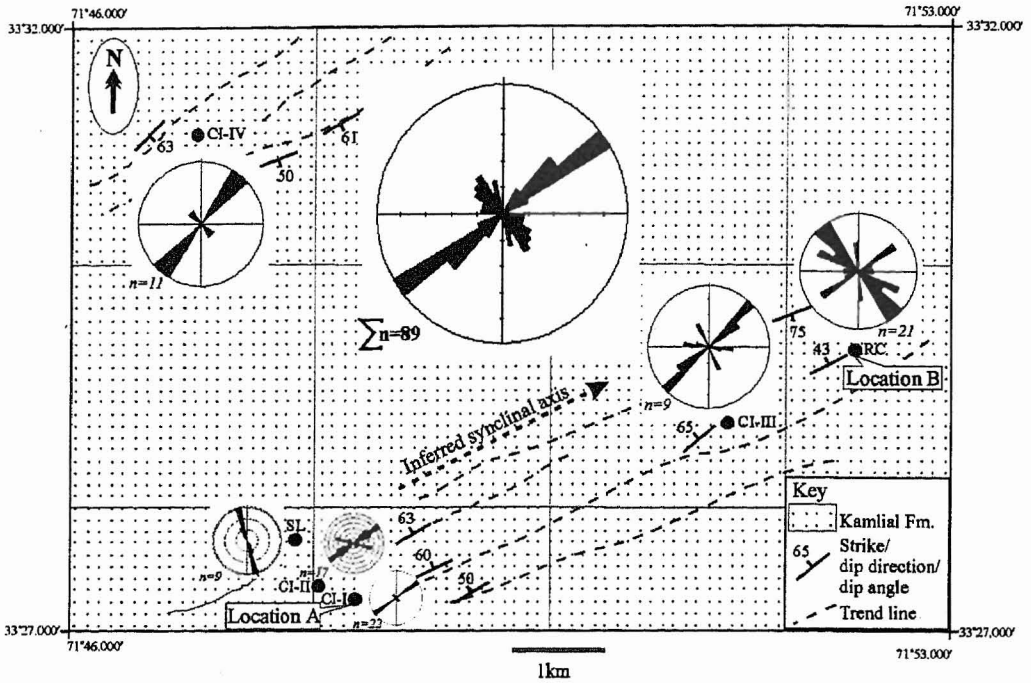

Fig. 9. Fracture pattern in the Kamlial Formation of the Khushalgarh syncline. Note, that the NE-SW fractures follow the axis of the fold, whereas the NW-SE fractures cut fold axis at high angle. Inferred fold axis is after Searle & Khan (not dated). CI: circle inventory, SL: scanline, RC: rectangle.

We suggest that NE-SW trending fractures formed prior to NE-SW trending fractures. However, both sets appear to be synchronous with the folding event. From the NE-SW fracture mode, which oriented orthogonal to the bedding, we conclude that the sandstone units underwent at least bedding-parallel extension during folding, where bedding is stretched to accommodate extension, parallel to the fold axis orientation. Thus, bending of the limbs is a likely mechanism for the development of observed NE-SW trending fractures. However, some of these fractures were locally reactivated in shear, thereby accommodating minor shear offsets. Based on crosscutting relationship, we suggest that the NW-SE trending shear fractures are not synchronous to the NE-SW set, however, both the sets are synchronous with the folding (Fig. 8b). The orientation and formation of these fracture sets are consistent with the regional stress regime of the Himalayan foreland (cf. Figs. 1 & 9).

DISCUSSION AND CONCLUSIONS

Testing existing conceptual fold-fracture models

Stearns (1968) proposed that there are five fracture sets that form systematically with respect to the fold axis and bedding. Each set comprised of two shear fractures and one extension fracture. This model assumes that all three possible fracture orientations of each set can form simultaneously. This assumption, however, contradicts laboratory observations suggesting that usually only one fracture orientation forms in a sample (e.g., Griggs & Handin, 1960).

Based on the orientation of the fractures, cross cutting relationships and their modes in response to stress, we conclude that NE-SW trending fractures formed early than those of NW-SE set. Though, both the fracture sets are formed during the folding, we suggest that they were not formed at the same time as suggested by Stearns (1968). Their cross cutting relationship further suggests that they developed sequentially rather than synchronously. Our interpretations support the laboratory-based models where only one fracture orientation (or set of fractures with one orientation) form in response to single stress. Because of the change in the strain conditions of the sandstone beds during folding in response to the stress, new fractures of distinct orientations can form. The new set not only abuts the older set, but can also accommodate the strain in response to stress.

Acknowledgements: The authors would like to acknowledge Ghazanfar A. Khattak, Saqib Paracha, Rizwan Bari and Jasim Ashraf for assistance in the field. Funding for this work was provided by the NCE in Geology, University of Peshawar. The author would like to acknowledge an anonymous reviewer for his valuable comments. Special thanks to Mohammad Khan (driver) for helping in finding the routes in the Khushalgarh.

REFERENCES

Berg, S.S. & Skar, T., (in press). Controls on damage zone asymmetry of a normal fault zone: outcrop analyses of a segment of the Moab fault, SE Utah. Jour. of Struct. Geol.

Billi, A., (in press). Attributes and influence on fluid flow of fractures in foreland carbonates of southern Italy. J. Struct. Geol.

Billi, A. & Salvini, F., 2003. Development of systematic joints in response to flexure-related fibre stress in flexed foreland plates: the Apulian forebulge case history, Italy. J. Geody., 36, 523-536.

Dholakia, S.K., Aydin, A., Pollard, D.D. & Zoback, M.D., 1998. Fault-controlled hydrocarbon pathways in the Monterey Formation, CA. Am. Assoc. of Pet. Geol. Bull., 82, 1551-1574.

Griggs, D.T. & Handin, J., 1960. Observations on fracture and an hypothesis of earthquakes. In: Rock deformation, Boulder, Colorado (D.T. Griggs & J. Handin, eds). Geol. Soci. of Am. Mem., 79, 347-364.

Jaswal, T.M., Lillie, R.J. & Lawrence, R. D., 1997. Structure and evolution of the Northern Potwar Deformed Zone, Pakistan. Am. Assoc. Petrol. Geol. Bull., 81, 308-382.

Peacock, D.C.P., Knipe, R.J. & Sanderson, D.J., 2000. Glossary of normal faults. J. Struct. Geol., 22, 291-305.

Price, N.J. & Cosgrove, J.W., 1990. Analysis of geological structures. Cambridge University Press, Cambridge, 502.

Searle, M.P. & Khan, M.A (1995). Geological map of North Pakistan.

Stearns, D.W., 1968. Certain aspects of fractures in naturally deformed rocks. In: Rock mechanics seminar, Bedford (R.E. Riecker, ed). Terrestrial Sci. Lab., 97-118.

Twiss, R.J. & Moores, E.M., 1992. Structural Geology. Freeman, New York, 532.